Int. J. Electrochem. Sci., 7 **(2012)** 4397 - 4404

International Journal of
ELECTROCHEMICAL
SCIENCE
www.electrochemsci.org

In-situ Preparation and Electrochemical Performance of an Urchin-like Carbon Nanofibers@$LiFePO_4$ Hybrid

Xinlu Li[1,*], *Hao Wang*[1], *Hongfang Song*[1], *Hongyi Li*[1], *Jiamu Huang*[1], *Seong-ho Yoon*[2], *Feiyu Kang*[3]

[1] School of Materials Science and Engineering, Chongqing University, Chongqing, 400030, China
[2] Institute for Materials Chemistry and Engineering, Kyushu University, Kasuga, 8168580, Japan
[3] Advanced Materials Institute, Graduate School at Shenzhen, Tsinghua University, Shenzhen,518055, China
[*]E-mail: lixinlu@cqu.edu.cn

Received: 9 March 2012 / *Accepted:* 11 April 2012 / *Published:* 1 May 2012

Carbon nanofibers are in-situ prepared on the surface of $LiFePO_4$ by chemical vapor deposition, resulting in an "urchin-like" hybrid. The microstructure of the nanocomposite is analyzed by XRD, TEM, SEM and N_2 absorption. TEM images show that the carbon nanofibers are amorphous with less than 100 nanometers in diameter. The specific surface area increase remarkably when carbon nanofibers are in-situ grown on the surface of $LiFePO_4$. The cycle performance is investigated by galvanostatic charge-discharge tests at different rate. The reversible capacity of $LiFePO_4$ is improved effectively when carbon nanofibers are oriented on the surface. Compared to the bare $LiFePO_4$, the discharge capacity of carbon nanofibers@$LiFePO_4$ increase to 162 mAh g^{-1} at 0.1 C rate. Electrochemical impedance spectra prove that the orientation of carbon nanofibers is effective to improve the electron conductivity. Cyclic voltammograms display no cathodic peaks for the reaction of Ni catalyst with Li^+ in the charge-discharge process.

Keywords: Carbon nanofibers; Chemical vapor deposition; Cathode materials; Lithium ion batteries

1. INTRODUCTION

Recently, $LiFePO_4$ has captured extensive attention as a promising cathode material for lithium-ion batteries due to its high energy density, low cost and environmental friendliness. It is known that electron removal occurs simultaneously and repeatedly in the process of Li^+ intercalation/de-intercalation from the cathode materials of lithium ion batteries. As a result, both ionic and electronic conductivity are critically important to cathode active materials, especially at fast rate. However, $LiFePO_4$ is quite poor in electron conductivity (around 10^{-6}-10^{-9} S cm^{-1}) [1]. Usually, about 10-20 wt% of carbon black is added in the $LiFePO_4$ cathode preparation to improve the electron

conductivity [2, 3]. Other efforts have also been made to overcome the drawback, such as reducing the particle size [4], cation doping with Ni^{2+} or Mg^{2+} [5-7] and surface coating with conducting polymer or carbon [8, 9].

Whittingham et al. added carbon nanotubes (CNTs) in the synthesis process of $LiFePO_4$ in attempt to increase the conductivity [10, 11]. Li et al. mixed $LiFePO_4$ with well-crystallized CNTs in the cathode preparation. It was found that $LiFePO_4$ particles were interwined by CNTs to form a three-dimensional network [12, 13]. Xu et al reported that $LiFePO_4$ were coated with CNTs through a hydrothermal route followed by heat treatment [14]. The elctrochemical examinations showed that the $LiFePO_4$-CNTs samples have higher discharge capacity and better cycle performance than as-prepared $LiFePO_4$. Besides, Bhuvaneswari et al. reported that carbon nanofibers (CNFs) were coated on $LiFePO_4$ particles by a non-aqueous sol–gel technique [15]. Recently, Li et al [16] prepared an urchin-like graphite-based anode material by chemical vapor deposition for lithium ion batteries. It was found that in-situ growth of CNTs on the surface of graphite was effective to improve the reversible capacity at fast rate. However, there are no reports on the in-situ preparation of CNFs on the surface of $LiFePO_4$. Undoubtedly, $LiFePO_4$ and CNFs would form a nanocomposite together if CNFs are oriented on the surface directly instead of mixing or coating. If so, the conductivity of the cathode materials would be improved greatly, facilitating the electrochemical reactions of Li^+ intercalation/de-intercalation.

Herein, we introduce the in-situ preparation of an urchin-like CNFs@$LiFePO_4$ hybrid by chemical vapor deposition (CVD). The investigation is focused on the effect of in-situ growth of CNFs on the microstructure and electrochemical performance of $LiFePO_4$.

2. EXPERIMENTAL

The $LiFePO_4$ sample was provided by JingRui Battery Co. Ltd. (Guangzhou, China), of which the average particle size (D50) was 4.75 μm, and lattice parameter *a*, *b* and *c*, was 0.608 nm, 1.033 nm and 0.469 nm, respectively. The urchin-like $LiFePO_4$-based hybrid was synthesized by CVD method. First, $Ni(NO_3)_2$•$6H_2O$ was mixed with $LiFePO_4$ in 1:100 weight ratio in ethanol solvent. Second, the ethanol was evaporated completely in a rotary evaporator at 50 ^oC. Finally, the $LiFePO_4$ loaded with $Ni(NO_3)_2$•$6H_2O$ was put homogeneouly on a Si boat (40 ×80 mm), which was placed in the center of the heating zone (around 300 mm long) in a quartz tube (60 mm diameter and 800 mm long). The sample was heated at 500 ^oC for 30 min in Ar/H_2 (120 / 40 sccm) gas flow, then in C_2H_4/H_2 (120 / 40 sccm) gas flow for 30 min at 10 Torr pressure. The CNFs@$LiFePO_4$ was formed in the final step.

Phase structure of $LiFePO_4$ was analyzed by powders X-ray diffraction (XRD) using Rigaku diffractometer (D/Max-RB) with Cu Kα radiation. The scanning angle range (2θ) was from 15° to 70° with the scanning rate of 4°/min. Scanning electron microscopy (SEM, JSM 6700F) and high resolution transmission electron microscopy (HRTEM, LIBRA 200FE) were used to observe the morphology of the urchin-like hybrid. Specific surface area and porosity structure were measured by nitrogen adsorption/de-adsorption using an automatic adsorption system (ASAP 2020 M+C).

The working electrode was prepared by mixing CNFs@$LiFePO_4$ and polyvinylidone difluoride in 90:10 weight ratio in N-methyl-2-pyrrolidone (NMP) solvent. In the case of bare sample, the cathode was prepared by mixing $LiFePO_4$, carbon black and polyvinylidone difluoride in the weight ratio 80:10:10 in NMP solvent. The cathode loading of $LiFePO_4$ on Al foil was 0.753 mg/cm^2. Charge-discharge characteristics were examined with CR2032 coin cells, which were assembled in an argon-filled glove box. These cells were composed of a lithium foil as the anode, 1 M $LiPF_6$ in the volume ratio of 1:1 ethyl methyl carbon (EMC)/dimethyl carbonate (DMC) as the electrolytes, microporous polyethylene separator (Celgard 2400) and the prepared cathode. These cells were charge-discharged galvanostatically on LAND 2001 CT battery tester. Cyclic voltammetry (CV) was carried out at 0.01 mV s^{-1} scanning rate in the potential range from open circuit voltage to 4.2 V vs. Li/Li^+. Electrochemical impedance spectrascopy (EIS) was performed from 0.1 Hz to100 kHz using Solartron (1260 8w).

3. RESULTS AND DISCUSSION

Both the SEM and TEM images show the morphology of the CNFs@$LiFePO_4$ hybrid. Fig. 1(a) illustrates that CNFs are oriented radially on the surface of $LiFePO_4$ after CVD process, resulting in an urchin-like CNFs@$LiFePO_4$ hybrid.

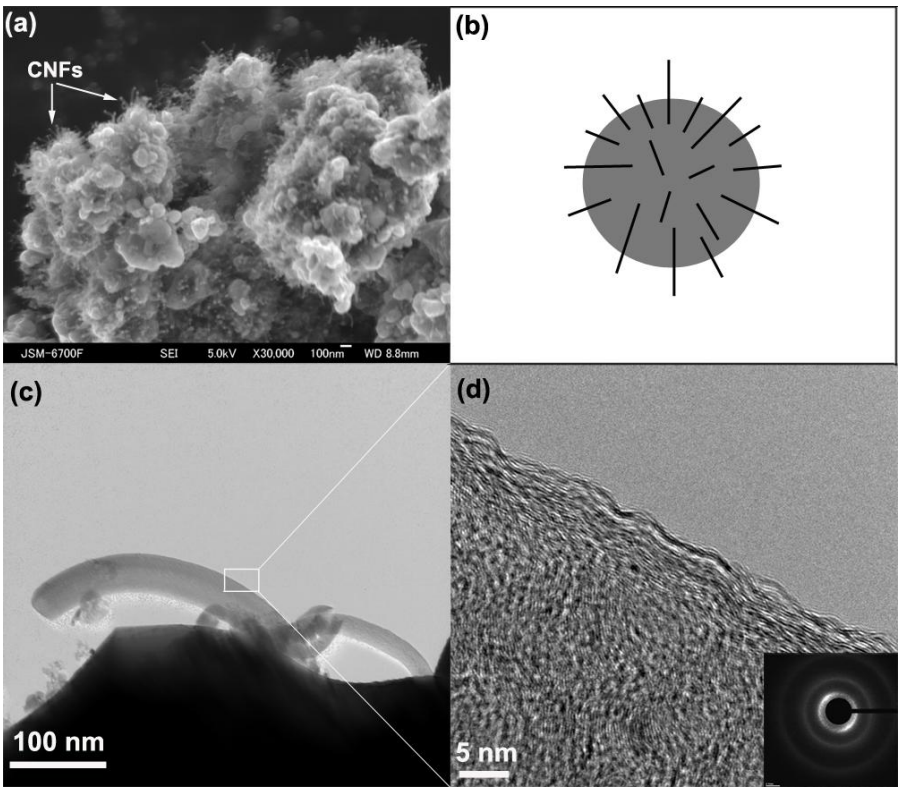

Figure 1. (a) SEM image of CNFs@$LiFePO_4$, (b) A structure model of the urchin-like nanocomposite, (c) HRTEM images of CNFs@$LiFePO_4$, (d) The enlarged image of the rectangle in (c).

As seen in Fig. 1(b), the $LiFePO_4$ particles could be viewed as "the core" while CNFs could be viewed as the radial "thorns" on the surface. This structure is like neither the three-dimensional network by CNTs interwining [12, 13] nor the core-shell structure by surface coating [8, 9]. Fig. 1(c) shows that the CNFs are oriented on the surface of $LiFePO_4$, of which the diameter is less than 100 nm. In Fig. 1(d), both the magnified image and the electron diffusion rings of the selected area confirm that the CNFs are amorphous. The content of CNFs is calculated to be 13.3 wt% in the final product according to the increased weight of the resultant after CVD at 500 ^oC for 30 min in C_2H_4/H_2 atmosphere. The weight of Ni catalyst is calculated to be 0.17 wt% on the $LiFePO_4$ according to the decomposition reaction of $LiFePO_4$ loaded with 1wt% $Ni(NO_3)_2$ after heat treatment at 500 ^oC for 30 min in Ar/H_2 (120 sccm/ 40 sccm) atmosphere.

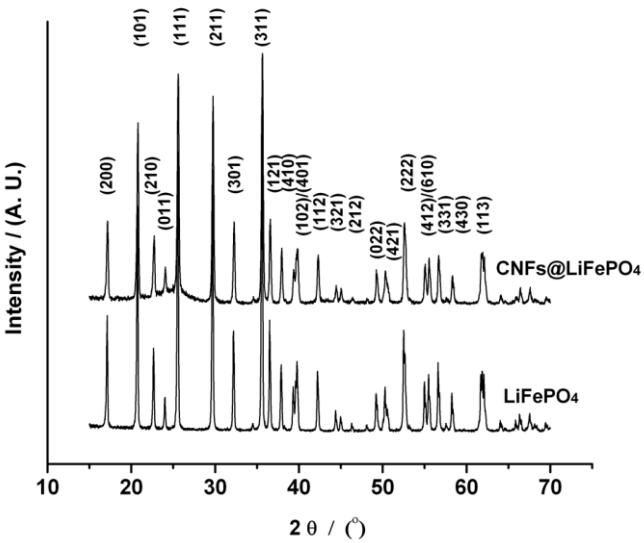

Figure 2. XRD patterns of the bare $LiFePO_4$ and CNFs@$LiFePO_4$.

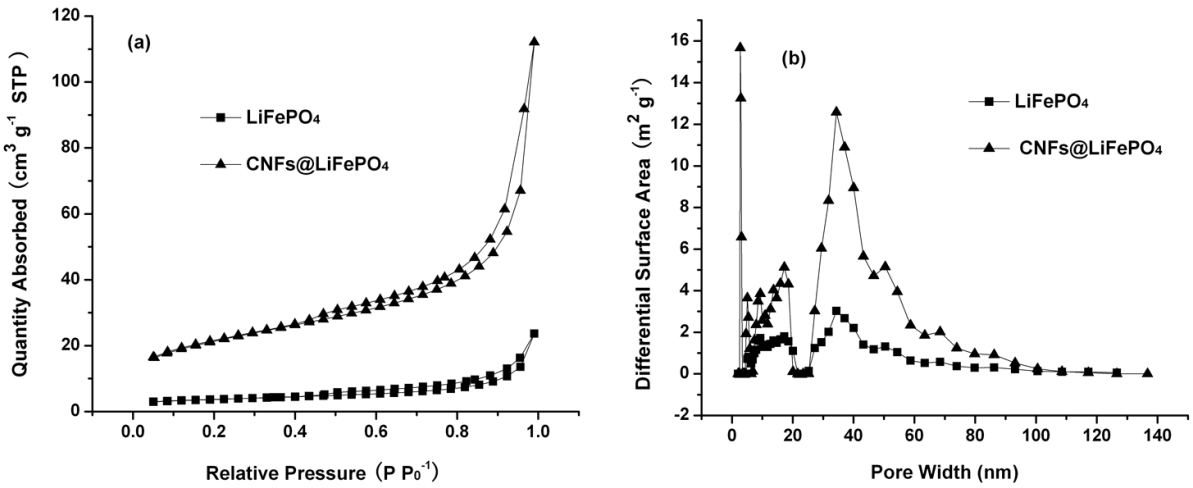

Figure 3. Nitrogen adsorption/de-adsorption curves of the bare $LiFePO_4$ and CNFs@$LiFePO_4$.

In Fig.2, both XRD patterns ranging from 15° to 70° for $LiFePO_4$ before and after CVD maintain the same, proving that the ovline-type crystal structure of $LiFePO_4$ does not change after CVD process. The diffraction peak at 2θ=26º confirm that the structure of CNFs on the surface of $LiFePO_4$ are amorphous.

Fig. 3(a) shows the nitrogen adsorption–desorption isotherms. The increase in quantity absorbed indicates the remarkable enhancement of specific surface area when CNFs are oriented on the surface of $LiFePO_4$. This phnomenon was also observed in the case of the urchin-like CNTs@graphite [16]. The BET specific surface area of the original $LiFePO_4$ was 12.55 m^2 g^{-1} and the average porosity width was 11.7 nm. After CVD process, the corresponding data changed to be 74.46 m^2 g^{-1} and 9.3 nm, respectively. Fig. 3(b) illustrates that the mesopores less than 50 nm in diameter increases greatly in the case of CNFs@$LiFePO_4$, leading to the striking increase in specific surface area.

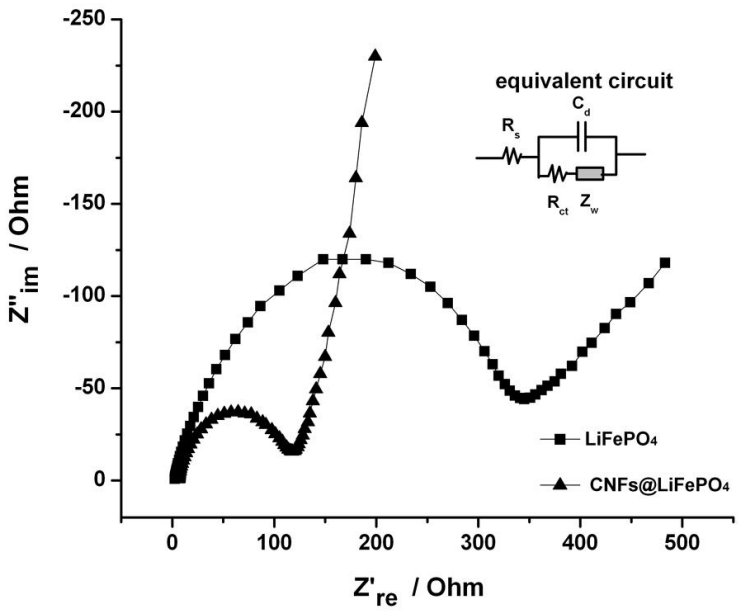

Figure 4. EIS spectra of both fresh $LiFePO_4$ and CNFs@$LiFePO_4$ electrode in three-electrode configuration in 1 M $LiPF_6$/EMC-DMC (1:1 in v v^{-1}) in the frequency range from 0.1 Hz to100 kHz.

Fig. 4 presents the Nyquist plots of the bare $LiFePO_4$ and CNFs@$LiFePO_4$ electrode. Both the EIS spectra are combinations of a semicircle in high frequencies and a straight line in low frequencies. The impedance spectra can be explained on the basis of the equivalent circuit on the right. The symbols in the equivalent circuit Rs, Rct, Cd, and Zw denote the solution resistance, charge-transfer resistance, capacitance of the double layer, and Warburg impedance, respectively. The diameter of the semicircle is attributed to the interfacial charge transfer resistance (R_{ct}) of electrochemical reactions and the line to the diffusion controlling Warburg impedance [14, 17]. In the medium frequency region, the intercepts with real impedance [Re(Z)] axis of the bare $LiFePO_4$ and CNFs@$LiFePO_4$ is 341 Ohm and 116 Ohm, respectively. The decrease in the semicircles is attributed to the increase in the effective

electrochemical interface by improved electron supply. This phenomenon is caused by the orientation of CNFs on the surface of $LiFePO_4$, which will facilitate the fast charge transfer between the electrolyte and the solid $LiFePO_4$ [17].

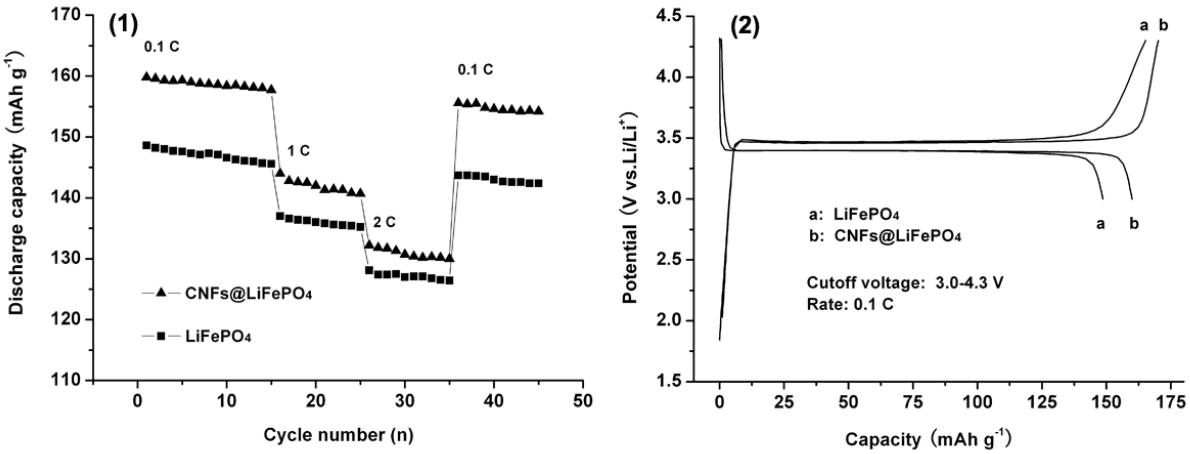

Figure 5. (1) Cycle performance of CNFs@$LiFePO_4$ and $LiFePO_4$ in 1 M $LiPF_6$/EMC-DMC (1:1 in v v^{-1}) at different charge-discharge rate, (2) The initial charge-discharge curves of CNFs@$LiFePO_4$ and $LiFePO_4$.

As illustrated in Fig. 5(1), the reversible capacity of CNFs@$LiFePO_4$ is higher than that of bare sample. The discharge capacity of CNFs@$LiFePO_4$ is 162 mAh g^{-1} at 0.1 C rate, 144 mAh g^{-1} at 1 C rate and 132 mAh g^{-1} at 2 C rate at the 3.0-4.3 V cutoff voltage, respectively. Correspondingly, the discharge capacity of the bare sample is 149 mAh g^{-1} at 0.1 C rate, 137 mAh g^{-1} at 1 C rate and 128 mAh g^{-1} at 2 C rate. In Fig. 5(2), the initial charge-discharge plateau of CNFs@$LiFePO_4$ becomes larger than that of bare sample. In the case of CNFs@$LiFePO_4$, the initial cycle efficiency increases to 94% and the stability in 15 cycles improves to 98.9% at 0.1 C rate (0.2 mA cm^{-2} current density). According to previous literature, the discharge capacity of $LiFePO_4$ coated with CNFs was about 140 mAh g^{-1} at 0.1 C rate when 10 wt% CNFs were coated on the surface of $LiFePO_4$ by a sol-gel method [15]. And Xu et al reported that $LiFePO_4$ coated with CNTs (5wt.%) exhibited an initial discharge capacity of 160 mAh g^{-1} at 0.3 C and the capacity fading was 0.4% after 50 cycles [14]. In addition, Li et al. found that the discharge capacity of $LiFePO_4$ mixed with 5 wt% CNTs was 155 mAh g^{-1} at 0.1 C [12]. The discharge capacity of CNFs@$LiFePO_4$ at different rate seem to be higher than that of $LiFePO_4$ mixed with CNTs or coated with CNFs in the condition that the quanlity of $LiFePO_4$ were the same.

Cyclic voltammetry was performed in order to investigate the effect of the orientation of CNTs on the electrochemical reaction mechanism of $LiFePO_4$. Fig. 6 shows the CV curves for the CNFs@$LiFePO_4$ in the first two cycles. It is found that the CNFs@$LiFePO_4$ electrode demonstrates only one couple of anodic/cathodic peaks, excluding the extra peak for the reaction of Li^+ with Ni

residue from open circuit voltage to 4.2 V vs. Li/Li^+. The CV curves prove that Li^+ does not react with the Ni catalyst in the charge-discharge process.

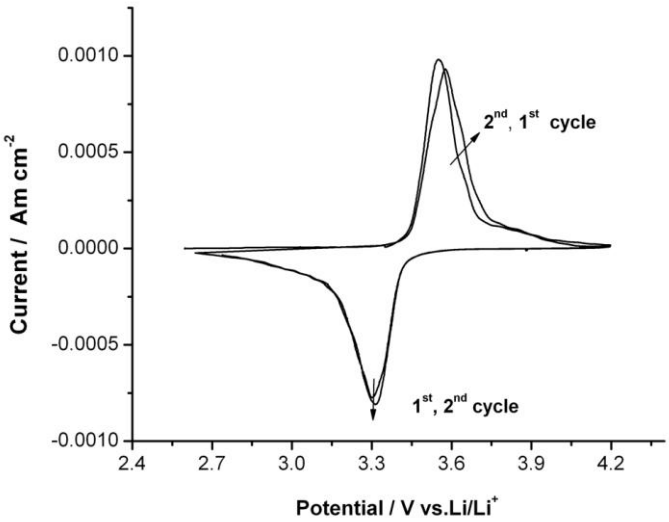

Figure 6. Cyclic voltammograms for the first 2 cycles obtained from CNFs@$LiFePO_4$ cathode in 1 M $LiPF_6$ / EMC-DMC (1:1 in v v^{-1}) at 0.01 mV s^{-1} scanning rate from open circuit voltage to 4.2 V vs. Li/Li^+.

The unique couple of redox peaks at the range of 3.3–3.5 V correspond to the two-phase nature of the lithium extraction and insertion reactions between $LiFePO_4$ and $FePO_4$ [3, 14]. In the second cycle, the cathodic peak has a slight shift to the higher potention and the anodic peak has a little shift to the lower direction. Both the sharpened peaks and the shortened potential interval prove the enhancement of the electrochemical reversibility of Li^+ intercalation/de-intercalation from CNFs@$LiFePO_4$. The well-defined peaks and narrower peak separation confirm the higher electrochemical reaction activity of CNFs@$LiFePO_4$ electrode.

4. CONCLUSION

In-situ preparation of CNFs on the surface of $LiFePO_4$ is accomplished by chemical vapor deposition, resulting in an "urchin-like" CNFs@$LiFePO_4$ nanocomposite. The CNFs are amorphous and the diameter is less than 100 nanometers. The specific surface area increase remarkably in the case of CNFs@$LiFePO_4$. The orientation of CNFs on the surface improves effectively the electrochemical reaction activity of Li^+ insertion/de-insertion from $LiFePO_4$. The discharge capacity of CNFs@$LiFePO_4$ is enhanced to 162 mAh g^{-1} at 0.1 C rate and 144 mAh g^{-1} at 1 C rate. The in-situ growth of CNFs effectively increases the electron conductivity of $LiFePO_4$ according to the decrease in the semicircles in high frequencies in the EIS spectra. The unique couple of anodic/cathodic peaks

in the CV curves prove that there are no reactions occur between Li^+ and Ni catalyst in the charge-discharge process from open circuit voltage to 4.2 V vs. Li/Li^+.

ACKNOWLEDGEMENT
The authors would like to thank the financial support from the Fundamental Research Funds for the Central Universities of China (No.CDJZR10 13 88 01 & No.CDJXS10 13 11 58) and National Natural Science Foundation of China (No.51172293). The authors also want to thank the technical support both from the Institute for Materials Chemistry and Engineering, Kyushu University, Japan and the Department of Materials Science and Engineering, Tsinghua University, China.

References

1. S. Y. Chung, J. T. Bloking and Y. M. Chiang, *Nature Mater.*, 1 (2002) 123.
2. V. Palomares, A. Goñi, I. G. d. Muro, I. de Meatza, M. Bengoechea, I. Cantero and T. Rojo, *J. Power Sources*, 195 (2010) 7661.
3. G. Wang, H. Liu, J. Liu, S. Qiao, G. M. Lu, P. Munroe and H. Ahn, *Adv Mater*, 22 (2010) 4944.
4. P. Prosini, *Electrochim. Acta*, 48 (2003) 4205.
5. P. S. Herle, B. Ellis, N. Coombs and L. F. Nazar, *Nature Mater.*, 3 (2004) 147.
6. E. M. Jin, B. Jin, D.-K. Jun, K.-H. Park, H.-B. Gu and K.-W. Kim, *J. Power Sources*, 178 (2008) 801.
7. Z. Liu, X. Zhang and L. Hong, *J. Appl. Electrochem.*, 39 (2009) 2433.
8. Y. Cui, X. Zhao and R. Guo, *J. Alloys and Compounds*, 490 (2010) 236.
9. M. Konarova and I. Taniguchi, *J. Power Sources*, 195 (2010) 3661.
10. J. Chen and M. Whittingham, *Electrochem. Commun.*, 8 (2006) 855.
11. L. W. Keqiang Ding, Jianjun Li, Haitao Jia, Xiangming He, *Int. J. Electrochem. Sci*., 6 (2011) 6165
12. X. Li, F. Kang, X. Bai and W. Shen, *Electrochem. Commun.*, 9 (2007) 663.
13. K. D. X.L. Li, H. Wang, H.F. Song, H.D. Liu, H.Y. Li, Y.X. Zhang, J.M. Huang *Int. J. Electrochem. Sci.*, 6 (2011) 4411
14. J. Xu, G. Chen and X. Li, *Mater. Chem. Phys.*, 118 (2009) 9.
15. M. S. Bhuvaneswari, N. N. Bramnik, D. Ensling, H. Ehrenberg and W. Jaegermann, *J. Power Sources*, 180 (2008) 553.
16. X. Li, S.-H. Yoon, K. Du, Y. Zhang, J. Huang and F. Kang, *Electrochim. Acta*, 55 (2010) 5519.
17. W. Zhang, X. Zhou, X. Tao, H. Huang, Y. Gan and C. Wang, *Electrochim. Acta*, 55 (2010) 2592